Published in final edited form as:

Am J Med Genet A. 2017 September ; 173(9): 2415–2421. doi:10.1002/ajmg.a.38349.

MED Resulting from Recessively-Inherited Mutations in the Gene Encoding Calcium-Activated Nucleotidase CANT1

Karthika Balasubramanian[1], **Bing Li**[1], **Deborah Krakow**[2,3,4], **Lisette Nevarez**[1], **Patric J. Ho**[1], **Julia A. Ainsworth**[1], **Deborah A. Nickerson**[5], **Michael J. Bamshad**[5,6], **University of Washington Center for Mendelian Genomics**[5], **LaDonna Immken**[7], **Ralph S. Lachman**[4], and **Daniel H. Cohn**[1,2,4]

[1]Department of Molecular, Cell and Developmental Biology, University of California Los Angeles, Los Angeles, California, USA

[2]Department of Orthopaedic Surgery, University of California Los Angeles, Los Angeles, California, USA

[3]Department of Human Genetics, University of California Los Angeles, Los Angeles, California, USA

[4]International Skeletal Dysplasia Registry, University of California Los Angeles, Los Angeles, California, USA

[5]Department of Genome Sciences, University of Washington, Seattle, Washington, USA

[6]Department of Pediatrics, University of Washington, Seattle, Washington, USA

[7]Specially For Children Genetics, Austin, Texas, USA

Abstract

Multiple Epiphyseal Dysplasia (MED) is a relatively mild skeletal dysplasia characterized by mild short stature, joint pain and early-onset osteoarthropathy. Dominantly inherited mutations in *COMP*, *MATN3, COL9A1, COL9A2,* and *COL9A3*, and recessively inherited mutations in *SLC26A2*, account for the molecular basis of disease in about 80–85% of the cases. In two families with recurrent MED of an unknown molecular basis, we used exome sequencing and candidate gene analysis to identify homozygosity for recessively inherited missense mutations in *CANT1*, which encodes calcium-activated nucleotidase 1. The MED phenotype is thus allelic to the more severe Desbuquois dysplasia phenotype and the results identify *CANT1* as a second locus for recessively inherited MED.

Correspondence: Daniel H. Cohn, Ph.D., Department of Molecular Cell and Developmental Biology, University of California, Los Angeles, TEL: 310-206-3990, dcohn@mcdb.ucla.edu.

WEB RESOURCES

Burrows Wheelers Aligner: http://bio-bwa.sourceforge.net/bwa.shtml#12
GATK: https://software.broadinstitute.org/gatk/
Picard: http://picard.sourceforge.net
dbSNP: https://www.ncbi.nlm.nih.gov/projects/SNP/
Exome Aggregation Consortium: http://exac.broadinstitute.org/
NHLBI Exome Sequencing Project Exome Variant Server: http://evs.gs.washington.edu/EVS/
NHLBI SeattleSeq Annotation: http://snp.gs.washington.edu/SeattleSeqAnnotation138/
OMIM: https://www.omim.org/

Keywords

Multiple epiphyseal dysplasia; CANT1; Skeletal dysplasia; Chondrodysplasia; Desbuquois dysplasia

INTRODUCTION

Multiple Epiphyseal Dysplasia (MED) is a chondrodysplasia that is characterized by mild short stature, joint pain, and early-onset osteoarthropathy, frequently resulting in joint replacement in the third or fourth decade of life [Bonafé et al., 2002; Briggs et al., 2003; Unger et al., 2008]. Radiographic features include epiphyseal dysplasia at the hips and knees, delayed carpal bone age and, in some cases, mild platyspondyly and irregularly-shaped vertebral bodies [Lachman et al., 2005]. Autosomal dominant mutations in *COMP* (OMIM 132400), *MATN3* (OMIM 607078), *COL9A1* (OMIM 120210), *COL9A2* (OMIM 600204), and *COL9A3* (OMIM 600969) account for the molecular basis of disease in ~70–75% of the cases [Jackson et al., 2012]. These genes encode structural proteins of the cartilage extracellular matrix (ECM) that are selectively expressed in the tissue [Zaucke F 2009]. A clinically distinct recessive form of the disease (rMED), which results from homozygosity or compound heterozygosity for mutations in *SLC26A2* (OMIM 226900), is characterized by epiphyseal dysplasia at the hips, advanced carpal ossification, and a double-layered patella that can be observed on a lateral x-ray of the knee. This rMED phenotype accounts for about 10–15% of MED cases [Superti-Furga et al., 1999], but may be higher in some populations [Jackson et al., 2012]. *SLC26A2* encodes a widely expressed sulfate transporter that imports inorganic sulfate into the cell for posttranslational protein sulfation [Haila et al., 2001; Satoh et al., 1998]. The molecular basis of MED remains unknown in ~15–20% of the cases.

All of the proteins encoded by the known MED-associated genes are involved in maintaining the structural integrity of the cartilage ECM. For the autosomal dominant forms of MED, the mutations exert their phenotypic effect through a dominant negative mechanism, leading to reduced secretion of structurally abnormal proteins into the extracellular matrix as well as intracellular retention of the abnormal proteins within the rough endoplasmic reticulum (RER) [Blumbach et al., 2009; Blumbach et al., 2008; Chen et al., 2008; Cotterill et al., 2005; Fresquet et al., 2008]. In addition to disrupting the matrix, accumulation of abnormal proteins within the RER can induce an unfolded protein response and lead to secondary abnormalities, including chondrocyte apoptosis [Nundlall et al., 2010; Piróg-Garcia et al., 2007]. Mutations in *SLC26A2* result in reduced activity of the sulfate transporter, which ultimately leads to decreased sulfation of proteins, particularly chondroitin sulfate proteoglycans, and negatively affects the ECM [Hastbacka et al., 1996; Rossi et al., 1998].

In this study, exome sequencing followed by candidate gene analysis was used to search for the molecular basis of MED in cases without a mutation in a known gene. In two families in which there was recurrence of MED, homozygosity for pathogenic mutations was identified in *CANT1,* the gene encoding calcium-activated nucleotidase 1. The data demonstrate that the spectrum of allelic conditions due to mutations in *CANT1* includes a second, recessively

inherited form of MED that is clinically distinct from the allelic but more severe Desbuquois dysplasia (OMIM 613165) phenotype.

MATERIALS AND METHODS

Patients

All patient samples were obtained through the International Skeletal Dysplasia Registry (ISDR) at the University of California, Los Angeles. Written informed consent was provided by all subjects under an approved Institutional Review Board (IRB) protocol. The two families included in this study have International Skeletal Dysplasia Registry reference numbers R92–280 and R01–152. DNA was isolated (Qiagen) from whole blood or Epstein Barr Virus transformed patient lymphoblastoid cell lines. All methods employed in this study were approved under a UCLA Biosafety protocol.

Homozygosity Mapping

Homozygosity mapping to identify runs of homozygosity (ROH) was conducted for the affected siblings in family R92–280 (cases R92–280A and R92–280B) using genome-wide single nucleotide polymorphism (SNP) array data. Shared ROH regions between the siblings were used for downstream data analysis.

Exome Sequencing

Exome sequencing was performed at the University of Washington Center for Mendelian Genomics (UWCMG). Exome libraries were prepared and 100 bp paired-end read sequences were derived using the Illumina platform. Sequence data were aligned to the Human GRCh37 reference genome using the Burrows Wheelers Aligner (BWA) MEM algorithm [Li 2012], and reads were de-duplicated using Picard. All further data processing was completed as published using the Genome Analysis Tool Kit (GATK) [McKenna et al., 2010]. All libraries had a depth of coverage of >20× for at least 90% of the targeted bases. Bam files were then recalibrated and realigned around the insertions and deletions and variant calling was conducted using UnifiedGenotyper. Variant quality was assessed using the Variant Quality Score Recalibration tool with a general linearized model for both SNPs and indels.

A multisample VCF was generated and annotated using the SeattleSeq variant annotation server [Ng et al., 2009]. The returned annotation file was saved to a SQL database and merged with the VCF. All variants not targeting the exome or splice junction consensus sequences were excluded. Variant filtering was conducted under a recessive model both across the entire dataset and in combination with the ROH regions identified by homozygosity mapping in family R92–280.

Sanger Sequence and Candidate Gene Analysis

PCR products for Sanger sequence analysis were generated using Qiagen Hotstart Taq DNA polymerase and touchdown PCR. PCR primers were designed using Primer3 software [Koressaar and Remm 2007; Untergasser et al., 2012]. CANT1 primers were designed to include all coding exon(s) and 20 bp flanking the intron-exon splice junctions with the

exception of the first coding exon (exon 3; transcript NM_001159773.1), which was amplified in 2 PCR products with overlapping regions covering approximately 30–40 bp in the middle of the exon. PCR and sequencing primer sequences can be found in Supplemental Table SI. Variants identified by exome sequencing were confirmed by Sanger sequence analysis of PCR products, in both the forward and reverse directions, with the sequences analyzed using Sequencher 2.0. Sequences were aligned to the GRCh37 reference sequence on the UC Santa Cruz Genome Browser [Kent et al., 2002]. Candidate gene mutation screening of *CANT1* in family R01–152 was conducted using bidirectional sequence analysis of PCR products of the coding exons.

RESULTS

To identify the molecular basis of MED in a family (R92–280) with recurrence of the phenotype, exome sequence analysis was carried out for the two affected siblings and their parents (Fig. 1). The exome sequences of the affected individuals (R92–280A and R92–280B) were first filtered for variants in the known MED loci, excluding all six genes and indicating that MED in the family is likely to result from a mutation at a distinct locus. Genome wide SNP array data (not shown) identified two large ROH regions shared by the two affected individuals, consistent with unknown ancestral consanguinity between the parents and a recessively inherited phenotype due to homozygosity for a mutation inherited identically by descent. The exome data were therefore filtered to identify all missense, nonsense and splicing variants for which both affected individuals were homozygous and the unaffected parents heterozygous. As family R92–280 is of Latino ancestry, we used the Latino allele frequencies in the Exome Aggregation Consortium (ExAC) [Lek et al., 2015] to filter for rare variants. After excluding all of the variants with MAF≥0.01, variants in fifteen candidate genes were identified (Table I). All but one of the variants were within the two large ROH intervals shared by the affected siblings, a 34.5 Mb block at chromosome 3q12.1 containing 3 variants and a 22.1 Mb block at chromosome 17q25.3 containing 11 variants. Because MED is a chondrodysplasia, we then filtered the remaining candidate genes by eliminating those that were either not expressed in human fetal growth plate cartilage or expressed at a very low level (FPKM ≤ 1.5) [Marques et al., 2016]. This left *TOP3A*, *TMEM199*, *KIAA0100* and *CANT1*, all in the ROH region on chromosome 17, and *PLXND1* in the ROH region on chromosome 3, as the remaining candidate genes. Because mutations in *CANT1* are known to result in Desbuquois dysplasia (DBQD), we focused on the p.Ile171Phe variant in the gene and the possibility that MED in the family is allelic to the more severe DBQD chondrodysplasia phenotype.

The *CANT1* p.Ile171Phe missense variant was absent in dbSNP, the Exome Sequencing Project (ESP) database, and the ExAC database. The variant was predicted to be “possibly damaging” by PolyPhen [Adzhubei et al., 2010] with a modest CADD score [Kircher et al., 2014] of 16.92. The Ile171 residue lies in the middle of the second nucleotide conserved region and the p.Ile171Phe substitution is adjacent to two mutations (p.Ser168Ala and p.Asp169Asn), identified by a mutagenesis study targeting the Ca^{2+} binding site that resulted in 96–99% diminished enzymatic activity [Dai et al., 2004].

An assessment of the radiographic phenotype of the two affected individuals in the family demonstrated irregularly shaped capital femoral epiphyses and a short femoral neck which resembles the “Swedish key” appearance of the proximal femur that is characteristic of DBQD (Fig. 2). Other notable defects included anterior wedging of the vertebral bodies, small epiphyses at the knees with metaphyseal flare, and advanced carpal ossification in the hands, with the latter finding also observed in DBQD patients. However, neither of the two affected siblings exhibited joint dislocations, scoliosis, coronal clefts, or any of the hand anomalies (accessory ossification centers and/or delta phalanx) consistent with a diagnosis of DBQD (Table II). As the metacarpal and phalangeal lengths were normal, the observed radiographic phenotype was also distinguished from the less severe DBQD Kim variant. Finally, the MED cases did not exhibit the characteristic facies of DBQD nor were any neurological complications noted.

From the ISDR archive, we identified four additional unsolved MED cases with the “Swedish key” radiographic appearance of the proximal femurs, and used Sanger sequence analysis to screen *CANT1* for variants. In one case, R01–152A, homozygosity for the *CANT1* missense variant p.Val226Met was identified. This is a known pathogenic mutation that has primarily been observed in the compound heterozygous state in cases with the DBQD Kim variant [Furuichi et al., 2011]. The radiographic phenotype of MED patient R01–152 had some overlapping features with DBQD, including degenerative arthrosis of the hand and spine by 25 years of age (Fig. 2), but the overall phenotype was milder and clearly distinct from DBQD (Table II).

DISCUSSION

Recessively inherited mutations in *CANT1* were identified in two recurrent cases of MED. Mutations in *CANT1* are known to cause Desbuquois dysplasia (DBQD), which is characterized by severe short stature, joint dislocations, scoliosis, advanced carpal and tarsal ossification, accessory ossification centers in the hand, and a characteristic “Swedish key” appearance of the proximal femur on radiographs [Huber et al., 2009]. The DBQD phenotypic spectrum comprises three clinically distinct entities. Type I and Type II DBQD are distinguished based on the presence or absence of the accessory ossification centers distal to the second metacarpal, or a delta phalanx [Faivre et al., 2004], and the DBQD Kim variant is clinically distinguished by a milder overall phenotype and short metacarpals with relatively elongated phalanges [Kim et al., 2010]. While the MED patients in our cohort were selected based on presence of a “Swedish key” appearance of the proximal femurs, they were of mild short stature and did not have joint dislocations, distinguishing the MED phenotype from DBQD I and II. Furthermore, their hands were radiographically normal, with no evidence of either short metacarpals or elongated phalanges, distinguishing the phenotype from the DBQD Kim variant. Thus the MED phenotype due to *CANT1* mutations is clinically distinct from all forms of DBQD and expands the phenotypic spectrum associated with mutations in the gene to include a second, recessively inherited form of MED.

Homozygosity for the p.Val226Met missense mutation was identified in case R01–152A. The p.Val226Met mutation lies in the fourth nucleotide conserved region and it has been

demonstrated to reduce CANT1 nucleotidase activity to about 20% of the wild-type enzyme activity [Furuichi et al., 2011]. Eight families with the milder Kim variant have been reported to date, and four of these cases result from one loss-of-function mutation and the p.Val226Met missense mutation. Homozygosity for the missense change likely results in higher enzyme activity relative to DBQD Kim type, providing a possible explanation for why the less severe clinical and radiographic phenotype of MED results. Homozygosity for the p.Val226Met mutation has been reported in one DBQD Kim family, but radiographic data for a full comparison of the phenotype with the case reported here have not been published [Furuichi et al., 2011; Kim et al., 2010]. Prior to this study the p.Val226Met variant has only been identified in individuals of Japanese and Korean ethnicity [Dai et al., 2011; Furuichi et al., 2011]. As the MED family was of Latino ancestry, the same mutation may have occurred independently in this ethnic group.

The p.Ile171Phe missense mutation identified in the homozygous state in MED family R92–280 has not been reported previously and lies in the second nucleotide conserved region, adjacent to the Ca^{2+} binding site. Because the observed radiographic phenotype is similar among affected individuals in families R92–280 and R01–152, the p.Ile171Phe substitution might result in diminished enzyme activity at a level similar to what is observed for the p.Val226Met substitution.

From a mechanistic viewpoint, in the study by Nizon et al. in 2012, CANT1 localizes to the Golgi and is involved in the synthesis of glycosaminoglycans (GAG) and the posttranslational modification of proteoglycans. They demonstrated that fibroblasts in DBQD patients with loss-of-function *CANT1* mutations have diminished GAG synthesis due to the inability of CANT1 to metabolize UDP to UMP. The UMP is normally exchanged for UDP-sugars, which are required for the synthesis and elongation of GAG chains [Nizon et al., 2012]. Based on this function, we suggest that *CANT1* MED mutations have a milder but similar indirect effect on extracellular matrix (ECM) biosynthesis, as many ECM proteins have GAG posttranslational modifications that may depend on wild-type CANT1 activity. It is not clear, however, whether the phenotype results from a general effect on multiple posttranslationally modified proteins or is due to defects in the mature form of one or a few proteins.

In conclusion, exome sequencing and candidate gene analysis identified homozygosity for recessively inherited mutations in *CANT1* in two families with recurrent MED. The phenotype has some similarity to the allelic forms of DBQD, but the observed clinical and radiographic phenotype was clinically distinct, identifying *CANT1* as a second locus for a recessively inherited form of MED.

Supplementary Material

Refer to Web version on PubMed Central for supplementary material.

Acknowledgments

We thank the families who participated in this work. We are grateful to Drs. Jeffrey Esko, Anne Phan and Ryan J. Weiss for their input regarding this project. This study was supported in part by grants from the National Institutes

of Health (NIAMS R01AR062651 and RO1AR066124). Sequencing was provided by the University of Washington Center for Mendelian Genomics (UWCMG) which is funded by the National Human Genome Research Institute and the National Heart, Lung and Blood Institute Grant 1U54 HG006493. We thank the Joseph Drown Foundation and the March of Dimes for their support of the International Skeletal Dysplasia Registry. The authors have no conflicts of interest.

References

Adzhubei IA, Schmidt S, Peshkin L, Ramensky VE, Gerasimova A, Bork P, Kondrashov AS, Sunyaev SR. A method and server for predicting damaging missense mutations. Nat Meth. 2010; 7(4):248–249.

Blumbach K, Bastiaansen-Jenniskens YM, DeGroot J, Paulsson M, van Osch GJVM, Zaucke F. Combined role of type IX collagen and cartilage oligomeric matrix protein in cartilage matrix assembly: Cartilage oligomeric matrix protein counteracts type IX collagen–induced limitation of cartilage collagen fibril growth in mouse chondrocyte cultures. Arthritis & Rheumatism. 2009; 60(12):3676–3685. [PubMed: 19950300]

Blumbach K, Niehoff A, Paulsson M, Zaucke F. Ablation of collagen IX and COMP disrupts epiphyseal cartilage architecture. Matrix Biology. 2008; 27(4):306–318. [PubMed: 18191556]

Bonafé, L., Mittaz-Crettol, L., Ballhausen, D., Superti-Furga, A. Multiple Epiphyseal Dysplasia, Recessive. In: Pagon, RA.Adam, MP.Ardinger, HH.Wallace, SE.Amemiya, A.Bean, LJH.Bird, TD.Ledbetter, N.Mefford, HC.Smith, RJH., Stephens, K., editors. GeneReviews®. Seattle, WA: University of Washington; 2002.

Briggs, MD., Wright, MJ., Mortier, GR. Multiple Epiphyseal Dysplasia, Autosomal Dominant. In: Pagon, RA.Adam, MP.Ardinger, HH.Wallace, SE.Amemiya, A.Bean, LJH.Bird, TD.Ledbetter, N.Mefford, HC.Smith, RJH., Stephens, K., editors. GeneReviews®. Seattle, WA: University of Washington; 2003.

Chen T-LL, Posey KL, Hecht JT, Vertel BM. COMP mutations: Domain-dependent relationship between abnormal chondrocyte trafficking and clinical PSACH and MED phenotypes. Journal of Cellular Biochemistry. 2008; 103(3):778–787. [PubMed: 17570134]

Cotterill SL, Jackson GC, Leighton MP, Wagener R, Mäkitie O, Cole WG, Briggs MD. Multiple epiphyseal dysplasia mutations in MATN3 cause misfolding of the A-domain and prevent secretion of mutant matrilin-3. Human Mutation. 2005; 26(6):557–565. [PubMed: 16287128]

Dai J, Kim O-H, Cho T-J, Miyake N, Song H-R, Karasugi T, Sakazume S, Ikema M, Matsui Y, Nagai T, Matsumoto N, Ohashi H, Kamatani N, Nishimura G, Furuichi T, Takahashi A, Ikegawa S. A founder mutation of CANT1 common in Korean and Japanese Desbuquois dysplasia. J Hum Genet. 2011; 56(5):398–400. [PubMed: 21412251]

Dai J, Liu J, Deng Y, Smith TM, Lu M. Structure and Protein Design of a Human Platelet Function Inhibitor. Cell. 2004; 117(3):413.

Faivre L, Cormier-Daire V, Eliott AM, Field F, Munnich A, Maroteaux P, Merrer ML, Lachman R. Desbuquois dysplasia, a reevaluation with abnormal and “normal” hands: Radiographic manifestations. American Journal of Medical Genetics Part A. 2004; 124A(1):48–53. [PubMed: 14679586]

Fresquet M, Jackson GC, Loughlin J, Briggs MD. Novel mutations in exon 2 of MATN3 affect residues within the α–helices of the A-domain and can result in the intracellular retention of mutant matrilin-3. Human Mutation. 2008; 29(2):330–330.

Furuichi T, Dai J, Cho T-J, Sakazume S, Ikema M, Matsui Y, Baynam G, Nagai T, Miyake N, Matsumoto N, Ohashi H, Unger S, Superti-Furga A, Kim O-H, Nishimura G, Ikegawa S. CANT1 mutation is also responsible for Desbuquois dysplasia, type 2 and Kim variant. Journal of Medical Genetics. 2011; 48(1):32–37. [PubMed: 21037275]

Haila S, Hästbacka J, Böhling T, Karjalainen–Lindsberg M-L, Kere J, Saarialho–Kere U. SLC26A2 (Diastrophic Dysplasia Sulfate Transporter) is Expressed in Developing and Mature Cartilage But Also in Other Tissues and Cell Types. Journal of Histochemistry & Cytochemistry. 2001; 49(8): 973–982. [PubMed: 11457925]

Hastbacka J, Superti-Furga A, Wilcox WR, Rimoin DL, Cohn DH, Lander ES. Sulfate Transport in Chondrodysplasia,a. Annals of the New York Academy of Sciences. 1996; 785(1):131–136. [PubMed: 8702119]

Huber C, Oulès B, Bertoli M, Chami M, Fradin M, Alanay Y, Al-Gazali LI, Ausems MGEM, Bitoun P, Cavalcanti DP, Krebs A, Le Merrer M, Mortier G, Shafeghati Y, Superti-Furga A, Robertson SP, Le Goff C, Muda AO, Paterlini-Bréchot P, Munnich A, Cormier-Daire V. Identification of CANT1 Mutations in Desbuquois Dysplasia. The American Journal of Human Genetics. 2009; 85(5):706–710. [PubMed: 19853239]

Jackson GC, Mittaz-Crettol L, Taylor JA, Mortier GR, Spranger J, Zabel B, Le Merrer M, Cormier-Daire V, Hall CM, Offiah A, Wright MJ, Savarirayan R, Nishimura G, Ramsden SC, Elles R, Bonafe L, Superti-Furga A, Unger S, Zankl A, Briggs MD. Pseudoachondroplasia and multiple epiphyseal dysplasia: A 7-year comprehensive analysis of the known disease genes identify novel and recurrent mutations and provides an accurate assessment of their relative contribution. Human Mutation. 2012; 33(1):144–157. [PubMed: 21922596]

Kent WJ, Sugnet CW, Furey TS, Roskin KM, Pringle TH, Zahler AM, Haussler D. The human genome browser at UCSC. Genome Res. 2002; 12(6):996–1006. [PubMed: 12045153]

Kim O-H, Nishimura G, Song H-R, Matsui Y, Sakazume S, Yamada M, Narumi Y, Alanay Y, Unger S, Cho T-J, Park SS, Ikegawa S, Meinecke P, Superti-Furga A. A variant of Desbuquois dysplasia characterized by advanced carpal bone age, short metacarpals, and elongated phalanges: Report of seven cases. American Journal of Medical Genetics Part A. 2010; 152A(4):875–885. [PubMed: 20358597]

Kircher M, Witten DM, Jain P, O'Roak BJ, Cooper GM, Shendure J. A general framework for estimating the relative pathogenicity of human genetic variants. Nat Genet. 2014; 46(3):310–315. [PubMed: 24487276]

Koressaar T, Remm M. Enhancements and modifications of primer design program Primer3. Bioinformatics. 2007; 23(10):1289–1291. [PubMed: 17379693]

Lachman RS, Krakow D, Cohn DH, Rimoin DL. MED, COMP, multilayered and NEIN: an overview of multiple epiphyseal dysplasia. Pediatric Radiology. 2005; 35(2):116–123. [PubMed: 15503005]

Lek M, Karczewski K, Minikel E, Samocha K, Banks E, Fennell T, O'Donnell-Luria A, Ware J, Hill A, Cummings B, Tukiainen T, Birnbaum D, Kosmicki J, Duncan L, Estrada K, Zhao F, Zou J, Pierce-Hoffman E, Cooper D, DePristo M, Do R, Flannick J, Fromer M, Gauthier L, Goldstein J, Gupta N, Howrigan D, Kiezun A, Kurki M, Levy Moonshine A, Natarajan P, Orozco L, Peloso G, Poplin R, Rivas M, Ruano-Rubio V, Ruderfer D, Shakir K, Stenson P, Stevens C, Thomas B, Tiao G, Tusie-Luna M, Weisburd B, Won H-H, Yu D, Altshuler D, Ardissino D, Boehnke M, Danesh J, Roberto E, Florez J, Gabriel S, Getz G, Hultman C, Kathiresan S, Laakso M, McCarroll S, McCarthy M, McGovern D, McPherson R, Neale B, Palotie A, Purcell S, Saleheen D, Scharf J, Sklar P, Patrick S, Tuomilehto J, Watkins H, Wilson J, Daly M, MacArthur D. Analysis of protein-coding genetic variation in 60,706 humans. 2015 bioRxiv.

Li H. Exploring single-sample SNP and INDEL calling with whole-genome de novo assembly. Bioinformatics. 2012; 28(14):1838–1844. [PubMed: 22569178]

Marques F, Tenney J, Duran I, Martin J, Nevarez L, Pogue R, Krakow D, Cohn DH, Li B. Altered mRNA Splicing, Chondrocyte Gene Expression and Abnormal Skeletal Development due to SF3B4 Mutations in Rodriguez Acrofacial Dysostosis. PLOS Genetics. 2016; 12(9):e1006307. [PubMed: 27622494]

McKenna A, Hanna M, Banks E, Sivachenko A, Cibulskis K, Kernytsky A, Garimella K, Altshuler D, Gabriel S, Daly M, DePristo MA. The Genome Analysis Toolkit: A MapReduce framework for analyzing next-generation DNA sequencing data. Genome Research. 2010; 20(9):1297–1303. [PubMed: 20644199]

Ng SB, Turner EH, Robertson PD, Flygare SD, Bigham AW, Lee C, Shaffer T, Wong M, Bhattacharjee A, Eichler EE, Bamshad M, Nickerson DA, Shendure J. Targeted capture and massively parallel sequencing of 12 human exomes. Nature. 2009; 461(7261):272–276. [PubMed: 19684571]

Nizon M, Huber C, De Leonardis F, Merrina R, Forlino A, Fradin M, Tuysuz B, Abu-Libdeh BY, Alanay Y, Albrecht B, Al-Gazali L, Basaran SY, Clayton-Smith J, Désir J, Gill H, Greally MT, Koparir E, van Maarle MC, MacKay S, Mortier G, Morton J, Sillence D, Vilain C, Young I, Zerres K, Le Merrer M, Munnich A, Le Goff C, Rossi A, Cormier-Daire V. Further delineation of

CANT1 phenotypic spectrum and demonstration of its role in proteoglycan synthesis. Human Mutation. 2012; 33(8):1261–1266. [PubMed: 22539336]

Nundlall S, Rajpar M, Bell P, Clowes C, Zeeff L, Gardner B, Thornton D, Boot-Handford R, Briggs M. An unfolded protein response is the initial cellular response to the expression of mutant matrilin-3 in a mouse model of multiple epiphyseal dysplasia. Cell Stress and Chaperones. 2010; 15(6):835–849. [PubMed: 20428984]

Piróg-Garcia KA, Meadows RS, Knowles L, Heinegård D, Thornton DJ, Kadler KE, Boot-Handford RP, Briggs MD. Reduced cell proliferation and increased apoptosis are significant pathological mechanisms in a murine model of mild pseudoachondroplasia resulting from a mutation in the C-terminal domain of COMP. Human Molecular Genetics. 2007; 16(17):2072–2088. [PubMed: 17588960]

Rossi A, Kaitila I, Wilcox WR, Rimoin DL, Steinmann B, Cetta G, Superti-Furga A. Proteoglycan sulfation in cartilage and cell cultures from patients with sulfate transporter chondrodysplasias: Relationship to clinical severity and indications on the role of intracellular sulfate production. Matrix Biology. 1998; 17(5):361–369. [PubMed: 9822202]

Satoh H, Susaki M, Shukunami C, Iyama K-i, Negoro T, Hiraki Y. Functional Analysis of Diastrophic Dysplasia Sulfate Transporter. Journal of Biological Chemistry. 1998; 273(20):12307–12315. [PubMed: 9575183]

Superti-Furga A, Neumann L, Riebel T, Eich G, Steinmann B, Spranger J, Kunze J. Recessively inherited multiple epiphyseal dysplasia with normal stature, club foot, and double layered patella caused by a DTDST mutation. Journal of Medical Genetics. 1999; 36(8):621–624. [PubMed: 10465113]

Unger S, Bonafé L, Superti-Furga A. Multiple epiphyseal dysplasia: clinical and radiographic features, differential diagnosis and molecular basis. Best Practice & Research Clinical Rheumatology. 2008; 22(1):19–32. [PubMed: 18328978]

Untergasser A, Cutcutache I, Koressaar T, Ye J, Faircloth BC, Remm M, Rozen SG. Primer3—new capabilities and interfaces. Nucleic Acids Research. 2012; 40(15):e115. [PubMed: 22730293]

Zaucke FGS. Genetic mouse models for the functional analysis of the perifibrillar components collagen IX, COMP and matrilin-3: Implications for growth cartilage differentiation and endochondral ossification. Histology and Histopathology. 2009; 24(8):13. [PubMed: 19012240]

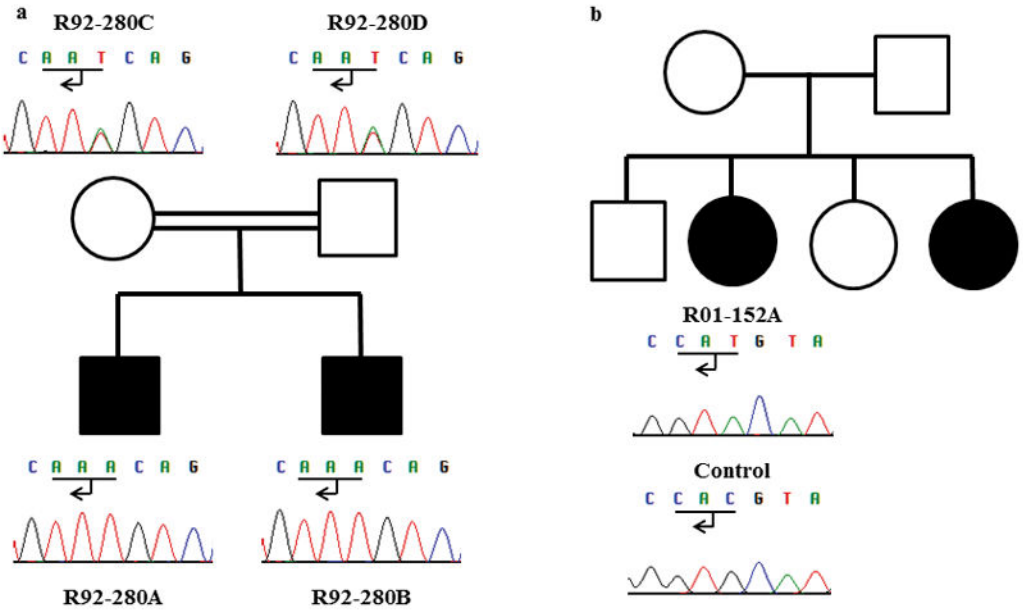

FIG. 1. MED Families with *CANT1* Mutations

(a) Family R92–280. Sanger sequencing demonstrated that the two unaffected parents (R92–280C and R92–280D) are carriers of variant p.Ile171Phe and the affected siblings (R92–280A and R92–280B) are homozygous for the variant. For each trace, the underline identifies the affected codon and the arrow indicates the direction of transcription. (b) Family R01–152. Individual R01–152A was homozygous for the p.Val226Met variant. DNA was not available from other family members.

FIG. 2. Radiographs of Patients with *CANT1* Mutations

(a–d) Radiographs of patient R92–280A at age 8. (a) AP pelvis shows flat, hypoplastic capital femoral epiphyses with flat acetabulae (left arrow) and mild Swedish key appearance of the proximal femur (right arrow). (b) Lateral lumbar spine showing minimal platyspondyly and anterior wedging/notching of the vertebral bodies, as indicated by the arrow. (c) AP hand shows no structural abnormality, but carpal age is advanced by 2 years. (d) AP knee showing small epiphyses with metaphyseal flare. (e–h) Radiographs of patient R01–152A at age 25. (e) AP right upper leg film shows epiphyseal dysplasia of the capital femoral epiphysis (right arrow) and a mild Swedish key, as indicated by the left arrow. (f) Lateral spine shows degenerative arthrosis (arrow). (g) AP hand showing degenerative arthrosis (carpal narrowing and periarticular osteoporosis). (h) AP knee revealing femoral medial-condylar epiphyseal dysplasia.

TABLE I

Homozygosity for Candidate Variants in Family R92–280

Chromosome	Gene	cDNA Change	Amino Acid Change	rsID	ExAC Latino MAF	PolyPhen Prediction	CADD Score
3	*GPR128*	c.800C>T	p.Ala267Val	--	0.0004319	benign	9.01
3	*CASR*	c.172G>C	p.Val58Leu	--	--	benign	12.49
3	*PLXND1*	c.3118C>G	p.Ala1040Pro	--	0.001613	benign	2.197
8	*OC90*	c.1339C>T	p.Glu447Lys	rs183454073	0.0002699	possibly-damaging	12.98
17	*TOP3A*	c.2224C>T	p.Asp742Asn	rs9909732	0.008891	benign	12.54
17	*TBC1D28*	c.167T>G	p.Glu56Ala	rs74452761	--	benign	7.143
17	*FBXW10*	c.1913G>A	p.Arg638Gln	rs143215236	0.0004319	probably-damaging	17.49
17	*TMEM199*	c.472C>A	p.Val158Ile	rs12572	0.00415	benign	19.73
17	*KIAA0100*	c.2958A>C	p.His986Gln	rs16964472	0.002418	benign	8.23
17	*SSH2*	c.3341G>C	p.Ala1114Gly	rs61737984	0.0009501	benign	1.389
17	*ATAD5*	c.5300A>G	p.Asn1767Ser	rs114345202	0.001994	benign	3.076
17	*LOC646021*	c.884A>G	p.His295Arg	rs149979077	--	unknown	0.12
17	*EVI2B*	c.853C>G	p.Asp285His	rs113483471	0.0007779	probably-damaging	17.8
17	*GPRC5C*	c.843G>C	p.Gln281His	rs370432099	0.003111	benign	3.408
17	*CANT1*	c.511T>A	p.Ile171Phe	--	--	possibly-damaging	16.92

TABLE II

Clinical and Radiographic Features of Disorders in the *CANT1* Phenotypic Spectrum

Feature	Type I DBQD	Type II DBQD	DBQD Kim Variant	R92–280A	R92–280B	R01–152	rMED *SLC26A2*
"Swedish Key"	+	+	+	+	+	+	−
Advanced Carpal Bone Age	+	+	+	+	+	NN	+
Accessory Ossification Centers	+	−	−	−	−	−	−
Delta Phalanx	+	−	−	−	−	−	−
Short Metacarpals	+	+	+	−	−	−	−
Elongated Phalanges	−	−	+	−	−	−	−
Coronal Clefts	+	+	−	−	−	−	−
Generalized Epiphyseal Dysplasia	+	+	+	+	+	+	+
Scoliosis	Severe	Severe	Severe	−	−	Mild	Mild
Joint Laxity/Dislocations	Multiple	Multiple	Multiple	−	−	−	−
Genu Varum	+	+	+	+	+	+	−
Club Foot	+	+	+	−	−	−	+
Distinctive Facies	+	+	+	−	−	−	−
Intellectual Disability	+	+	−	NN	NN	NN	−

+, feature present; −, feature absent; NN, Not Noted